Fast Level Set Segmentation of Biomedical Images using Graphics Processing Units

Hormuz Mostofi

Keble College

University of Oxford

Department of Engineering Science

Honour School of Engineering, Economics and Management

April 27, 2009

FINAL HONOUR SCHOOL OF
ENG / ECS / EEM (delete as appropriate)

DECLARATION OF AUTHORSHIP

You should complete this certificate. It should be bound into your fourth year project report, immediately after the title page. Three copies of the report should be submitted to the Chairman of Examiners for your Honour School, c/o Clerk of the Schools, Examination Schools, High Street, Oxford.

Name (in capitals):

College (in capitals): **Supervisor:**

Title of project (in capitals):

Page count: _____

Please tick to confirm the following:

I am aware of the University's disciplinary regulations concerning conduct in examinations and, in particular, of the regulations on plagiarism. ☐

The project report I am submitting is entirely my own work except where otherwise indicated. ☐

It has not been submitted, either wholly or substantially, for another Honour School or degree of this University, or for a degree at any other institution. ☐

I have clearly signalled the presence of quoted or paraphrased material and referenced all sources. ☐

I have acknowledged appropriately any assistance I have received in addition to that provided by my supervisor. ☐

I have not sought assistance from any professional agency. ☐

The project report does not exceed 50 pages (including all diagrams, photographs, references and appendices). ☐

I agree to retain an electronic version of the work and to make it available on request from the Chair of Examiners should this be required in order to confirm my word count or to check for plagiarism.

Candidate's signature: …….. Date: ……..

Contents

Chapter 1

Introduction

1.1 Image Segmentation

Image segmentation is the task of splitting a digital image into one or more regions of interest. It is a fundamental problem in computer vision and many different methods, each with their own advantages and disadvantages, exist for the task. Image segmentation is a particularly difficult task for several reasons. Firstly, the ambiguous nature of splitting up images into objects of interest provides a trade off between making algorithms more generalized or having many user specified parameters. Secondly, imaging artificats such as noise, inhomogeneities, acquisition artifacts and poor contrast, are very difficult to account for in segmentation algorithms without a high level of interactivity from the user.

In this report, segmentation is discussed in a medical imaging context however the proposed algorithm could equally be used in general purpose segmentations. Segmented images are typically used as the input for applications such as classification, shape analysis and measurement. In medical image processing, segmented images are used for studying anatomical structures, diagnosis and assisting in surgical planning.

Image segmentation also encompasses three dimensional volume segmentations, which are slower to compute by an order of magnitude. It should be noted that before such algorithms existed, segmentation of medical images was done by hand by experts. This was a very accurate, yet slow, process. These segmentations will form the gold standard with which to compare algorithmic segmentations.

In this report, the level set method is used for the purposes of segmentation. Their principal

disadvantage is that they are relatively slow to compute, which provides the motivation for optimizing and accelerating such algorithms using graphics processing units (GPUs). Section 3.1.1 discusses this further.

1.2 Parallel Processing

The algorithms for processing level sets have vast parallelization potential. Section 3.1 details the algorithms used to discretize the level set equation and Section 3.3 dicusses how these can be executed on graphics hardware.

1.2.1 GPGPU

General purpose computation on graphics processing units (GPGPU) is the technique of using graphics hardware to compute applications typically handled by the central processing unit (CPU). Graphics cards over the past two decades have been required to become highly efficient at rendering increasingly complex 3D scenes at high frame rates. This has forced their architecture to be massively parallel in order to be compute graphics faster than general purpose CPUs.

Compared to a CPU, a GPU features many more transistors on the control path due to the lower number of control instructions required. Memory is optimized for throughput and not latency, with strict access patterns. GPUs are not optimized for general purpose programs, and does not have the complex instruction sets, or branch control of the modern CPU. It should be noted however that modern CPUs feature multiple cores in order to take advantage of parallel processing.

The advent of GPGPU programming came with programmable shader units that allowed applying small programs to each pixel or vertex in the rendering pipeline. In order to write code to program the shader units, shading languages had to be used in conjunction with graphics APIs such as DirectX and OpenGL. NVIDIA developed the high-level shading language Cg to assist in programming shaders, however it still required knowledge of graphics APIs. More recently, languages have been developed that allow the programmer to implement algorithms without any knowledge of graphics APIs or architectures. One such language is NVIDIA CUDA, and is the language chosen for the optimizations in this project.

1.2.2 CUDA

Compute Unified Device Architecture, or CUDA, is NVIDIA's GPGPU technology that allows for programming of the GPU without any graphics knowledge. The C language model has at its core three key abstractions, from [15]: a heirarchy of thread groups. shared memories, and barrier synchronization. This breaks the task of parallelization into three sub problems, which allows for language expressivity when threads cooperate, and scalability when extended to multiple processor cores.

Framework

CUDA uses extends C by allowing a programming to write *kernels* that when invoked execute a thousands of lightweight identical threads in parallel. CUDA arranges these threads into a hierarchy of blocks and grids, as can be seen in Figure 1.1 allowing for runtime transparent scaling of code to different GPUs. The threads are identified by their location within the grid and block, making CUDA perfectly suited for tasks such as image processing where each threads is easily assigned to an individual pixel or voxel.

When writing and optimizing complex parallel code in CUDA it is often found that threads may need to cooperate. The memory hierarchy of CUDA threads is shown in Figure 1.2. Here it can be seen that each thread has access to: a per-thread private local memory, a per-block on-chip shared memory to share data between threads, and finally an off-chip global memory accessible to all threads within all blocks. There are also constant and texture memory spaces accessible to all threads, however these are not featured in our algorithm and so will not be discussed in any further detail.

Performance Guidelines

There are many techniques to optimize a parallel algorithm. Firstly, the optimum block and grid sizes should be used to ensure maximum 'occupancy'. Occupancy is the ratio of the number of active warps (32 parallel threads) to the maximum number of active warps supported by the GPU multiprocessor. To maximise efficiency, there is a trade off between making the occupancy very high, ensuring no multiprocessor is ever idle, and making it low enough to ensure no bank conflicts.

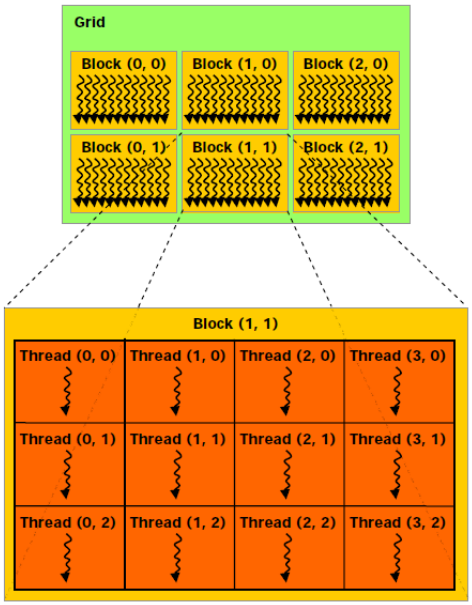

Figure 1.1: A grid of thread blocks. This figure is taken from [15]

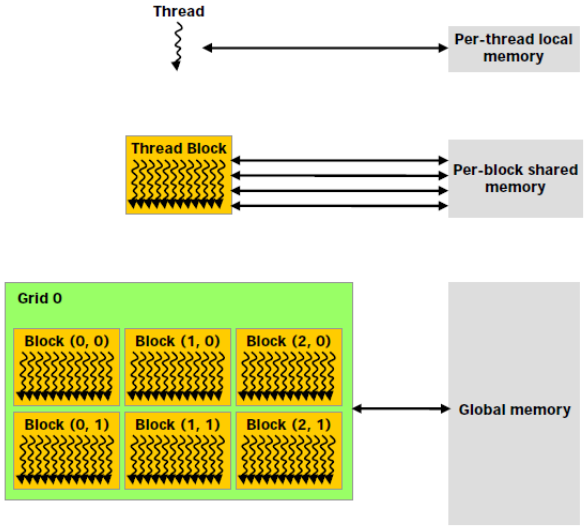

Figure 1.2: The memory hierarchy of CUDA threads and blocks. This figure is taken from [15]

Secondly, one of the best ways in which to optimize the parallelization is through efficient memory usage. The global memory space is not cached and therefore has a much higher latency and lower bandwidth than on-chip shared memory. Therefore it is the aim of the programmer to minimise global memory accesses. From [15], it recommended that each thread in a block firstly loads data from global memory to shared memory, synchronizes with all other threads within the thread block to ensure shared memory locations have been written to, processes the data, synchronizes again to ensure shared memory has been fully updated with results, and finally writes the results back to global memory coalesced.

Coalescence is an important concept in memory management as it can speed up memory reads and stores significantly. [15] lists the following three conditions for coalescing: "threads must access either 32-bit words, 64-bit words, or 128-bit words", "all 16 words must lie in the same segment of size equal to the memory transaction size" and "threads must access the words in sequence". Devices of higher *compute capability* feature incremental improvements to the core architecture, such as more relaxed requirements for coalescence (or support for double-precision floating point accuracy).

Chapter 2

Method

In this section, we introduce the level set method and dynamic implicit surfaces. Their role in segmentation is discussed having introduced and defined mathematical constructs such as signed distance transforms.

2.1 Level Set Method

The level set method evolves a contour (in two dimensions) or a surface (in three dimensions) implicitly by manipulating a higher dimensional function, called the level set function $\phi(\mathbf{x},\mathbf{t})$. The evolving contour or surface can be extracted from the zero level set $\Gamma(\mathbf{x},\mathbf{t}) = \{\phi(\mathbf{x},\mathbf{t}) = \mathbf{0}\}$. The advantage of using this method is that topological changes such as merging and splitting of the contour or surface are catered for implicitly, as can be seen below in Figure 2.1. The level set method, since its introduction by Osher and Sethian in [18], has seen widespread application in image processing, computer graphics (surface reconstructions) and physical simulation (particularly fluid simulation).

The evolution of the contour or surface is governed by a level set equation. The solution tended to by this partial differential equation is computed iteratively by updating ϕ at each time interval. The general form of the level set equation is shown below.

$$\frac{\partial \phi}{\partial t} = -|\nabla \phi| \cdot F \tag{2.1}$$

In the above level set equation F is the velocity term that describes the level set evolution. By manipulating F, we can converge the level set to different areas or shapes, given a particular

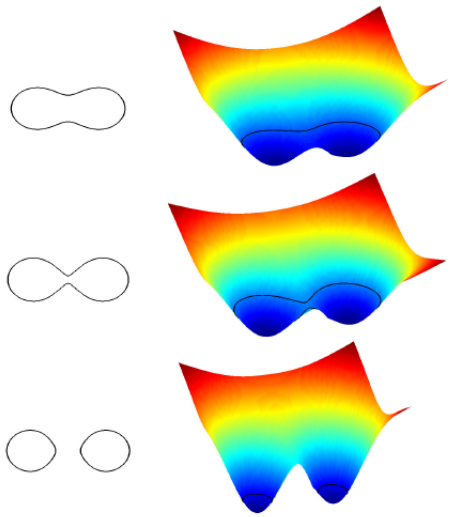

Figure 2.1: The relationship between the level set function (left) and contour (right) can be seen. It can be seen evolving the surface splits the contour.

initialisation of the level set function.

2.2 Segmentation using Level Sets

Typically, for applications in image segmentation F is dependent on the pixel intensity or curvature values of the level set. It may also be dependent on an edge indicator function, which is defined as having a value zero on an edge, and non-zero otherwise. This causes F to slow the level set evolution when on an edge.

In [12] F is dependent on data and curvature functions (with a weighting parameter between the two) for the purposes of image segmentation. Therefore, we will adopt the same methodology making the level set equation take the form

$$\frac{\partial \phi}{\partial t} = -|\nabla \phi| \left[\alpha D(\bar{x}) + (1-\alpha) \nabla \cdot \frac{\nabla \phi}{|\nabla \phi|} \right] \tag{2.2}$$

where the data function $D(I)$ tends the solution towards targeted features, and the mean curvature term $\nabla \cdot (\nabla \phi / |\nabla \phi|)$ keeps the level set function smooth. Weighting between these two is $\alpha \in [0, 1]$, a free parameter that is set beforehand to control how smooth the contour or surface should be.

The data function $D(I)$ acts as the principal 'force' that drives the segmentation. By making D positive in desired regions or negative in undesired regions, the model will tend towards the

segmentation sought after. A simple speed function that fulfills this purpose, used by Lefohn, Whitaker and Cates in [12, 2], is given by

$$D(I) = \epsilon - |I - T| \tag{2.3}$$

which is plotted in Figure 2.2. Here T describes the central intensity value of the region to be segmented, and ϵ describes the intensity deviation around T that is part of the desired segmentation. Therefore if a pixel or voxel has an intensity value within the $T \pm \epsilon$ range the model will expand, and otherwise it will contract.

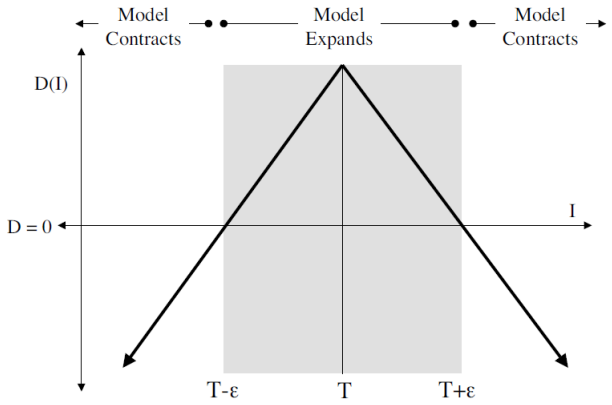

Figure 2.2: The speed term from [2]

Therefore the three user parameters that need to be specified for segmentation are T,ϵ and α. An initialization for the level set function is also required, which may take the form of a cube in three dimensions or a square in two dimensions, or any other arbitrary closed shape.

The importance of having a curvature term is shown in Figure 2.3. Here there is no force to smoothen high curvatures resulting in the contour *leaking*. This is when the level set surface evolves through a anatomical boundary into another anatomical object that was not intended to be segmented. This also makes segmentation tricky for objects which have very high curvature as the curvature weighting term often needs to be set very low in order to allow for these high curvatures, yet doing so may result in such leaking.

2.2.1 Signed Distance Transforms

A distance transform assigns a value for every pixel (or voxel) within a binary image containing one or more objects a value which represents the minimum distance from that pixel to the closest

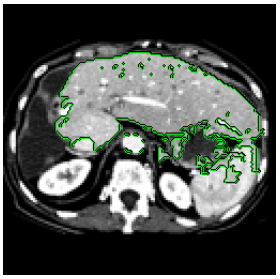

Figure 2.3: Leaking when there is no curvature term (or $\alpha = 1$)

pixel on the boundary of the object(s). The mathematical definition of a distance function $D : \mathbb{R}^3 \to \mathbb{R}$ for a set S, from [18], is

$$D(r, S) = \min|r - S| \text{ for all } r \in \mathbb{R}^3 \tag{2.4}$$

A *signed* distance transform assigns the sign of the distance value as positive for those pixels outside the object, and negative for those inside it. This is the sign convention that will be followed in the implementation, however the opposite sign convention is also used. It should be noted that the distance values depend on the chosen metric for distance: some common distance metrics are Euclidean distance, chessboard distance, and city block distance. Many of the algorithms that compute signed distance transforms often trade accuracy for efficiency and feature varying levels of complexity.

Signed distance transforms are required to initialize ϕ and also to reinitialize it every certain number of iterations. Computation of the initialization of ϕ is required before iteration of the level set equation can take place, and this will typically be a signed distance transform of an initial mask. Therefore the level set segmentation filter requires two images: an initial mask (which indicates targeted regions) and a *feature* image (which is the image to be segmented).

Alternatively, [8] provides a method of evolving level sets without reinitialization using signed distance transforms by forcing the level set function to be close to a signed distance function.

2.2.2 3D Volume Segmentations

Extending a two dimensional level set segmentation algorithm to three dimensions is a relatively straightforward task, however requires careful consideration of boundary conditions. In addition to the increased number of variables, creating a signed Euclidean distance function is one of

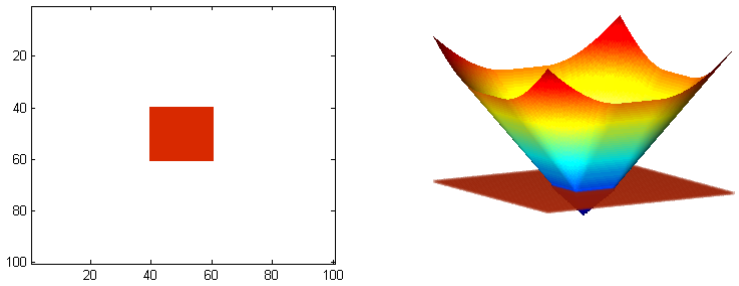

(a) Arbitrary Initial Mask

(b) Signed Distance Transform of Mask with Zero Level Set Overlaid

Figure 2.4: 2D Signed Euclidean Distance Transform

the major challenges in developing 3D segmentation code. Unfortunately, neither C code or CUDA code could be located to perform distance transform (re)initialisation in 3D and therefore MATLAB was used to initialise and reinitialise the level set during execution. There has however been recent work on CUDA accelerated distance transforms from [22],[5].

Chapter 3

Implementation

3.1 Level Set Algorithm

3.1.1 Upwinding

Equation (2.1), the level set equation, needs to be discretized for both sequential and parallel computation. This is done using the *up-wind* differencing scheme. The following explanation of *upwinding* is from [17].

A first order accurate method for time discretization of equation (2.1), is given by the forward Euler method, from [17]:

$$\frac{\phi^{t+\Delta t} - \phi^t}{\Delta t} + F^t \cdot \nabla \phi^t = 0 \tag{3.1}$$

where ϕ^t represents the current values of ϕ at time t, F^t represents the velocity field at time t, and $\nabla\phi^t$ represents the values of the gradient of ϕ at time t. When computing the gradient, a great deal of care must be taken with regards to the spatial derivatives of ϕ. This is best exemplified by considering the expanded form of equation (3.1).

$$\frac{\phi^{t+\Delta t} - \phi^t}{\Delta t} + u^t \phi_x^t + v^t \phi_y^t + w^t \phi_z^t = 0 \tag{3.2}$$

For simplicity, consider the one dimensional form of equation (3.2) at a specific grid point x_i

$$\frac{\phi^{t+\Delta t} - \phi^t}{\Delta t} + u_i^t (\phi_x)_i^t = 0 \tag{3.3}$$

where $(\phi_x)_i$ is the spatial derivative of ϕ at x_i. The method of characteristics indicates whether to use a forward or backwards difference method for ϕ based on the sign of u_i at the point x_i. If $u_i > 0$, the values of ϕ are moving from left to right, and therefore backwards difference methods (D_x^- in Equations 3.4) should be used. Conversely, if $u_i < 0$, forward difference methods (D_x^+ in Equations 3.4) should be used to approximate ϕ_x. It is this process of choosing which approximation for the spatial derivative of ϕ to use based on the sign of u_i that is known as *upwinding*.

Extending this to three dimensions, from [12], results in the derivatives below required for the level set equation update.

$$\begin{array}{lll} D_x = (u_{i+1,j,k} - u_{i-1,j,k})/2 & D_x^+ = u_{i+1,j,k} - u_{i,j,k} & D_x^- = u_{i,j,k} - u_{i-1,j,k} \\ D_y = (u_{i,j+1,k} - u_{i,j-1,k})/2 & D_y^+ = u_{i,j+1,k} - u_{i,j,k} & D_y^- = u_{i,j,k} - u_{i,j-1,k} \\ D_z = (u_{i,j,k+1} - u_{i,j,k-1})/2 & D_z^+ = u_{i,j,k+1} - u_{i,j,k} & D_z^- = u_{i,j,k} - u_{i,j,k-1} \end{array} \tag{3.4}$$

$\nabla\phi$ is approximated using the upwind scheme.

$$\nabla\phi_{\max} = \begin{bmatrix} \sqrt{\max(D_x^+,0)^2 + \max(-D_x^+,0)^2} \\ \sqrt{\max(D_y^+,0)^2 + \max(-D_y^+,0)^2} \\ \sqrt{\max(D_z^+,0)^2 + \max(-D_z^+,0)^2} \end{bmatrix} \tag{3.5}$$

$$\nabla\phi_{\min} = \begin{bmatrix} \sqrt{\min(D_x^+,0)^2 + \min(-D_x^+,0)^2} \\ \sqrt{\min(D_y^+,0)^2 + \min(-D_y^+,0)^2} \\ \sqrt{\min(D_z^+,0)^2 + \min(-D_z^+,0)^2} \end{bmatrix} \tag{3.6}$$

Finally, depending on whether $F_{i,j,k} > 0$ or $F_{i,j,k} < 0$, $\nabla\phi$ is

$$\nabla\phi = \begin{cases} ||\nabla\phi_{\max}||_2 & \text{if } F_{i,j,k} > 0 \\ ||\nabla\phi_{\min}||_2 & \text{if } F_{i,j,k} < 0 \end{cases} \tag{3.7}$$

$$\phi(t + \Delta t) = \phi(t) + \Delta t F|\nabla\phi| \tag{3.8}$$

The speed term F, as discussed before, is based on the pixel intensity values and curvature values.

This implementation is very computationally demanding (in terms of time taken and storage required) and therefore there have been several devlopments to optimize the implementation. Some of these include the narrow band method [1] and sparse field method [23]. The narrow band method restricts the computation of level set update to a thin band of 'active' pixel/voxels that are on or near to the level set implicit contour/surface. This speeds up computation as there is very little need to update the level set for pixel/voxels very far from the contour.

3.1.2 Curvature

Curvature is computed based on the values of the current level set using the derivatives below. In two dimensions only the first two derivatives are required, alongside the derivatives defined previously. In three dimensions, all the derivatives below are required.

$$\begin{aligned}
D_x^{+y} &= (u_{i+1,j+1,k} - u_{i-1,j+1,k})/2 & D_x^{-y} &= (u_{i+1,j-1,k} - u_{i-1,j-1,k})/2 \\
D_x^{+z} &= (u_{i+1,j,k+1} - u_{i-1,j,k+1})/2 & D_x^{-z} &= (u_{i+1,j,k-1} - u_{i-1,j,k-1})/2 \\
D_y^{+x} &= (u_{i+1,j+1,k} - u_{i+1,j-1,k})/2 & D_y^{-x} &= (u_{i-1,j+1,k} - u_{i-1,j-1,k})/2 \\
D_y^{+z} &= (u_{i,j+1,k+1} - u_{i,j-1,k+1})/2 & D_y^{-z} &= (u_{i,j+1,k-1} - u_{i,j-1,k-1})/2 \\
D_z^{+x} &= (u_{i+1,j,k+1} - u_{i+1,j,k-1})/2 & D_z^{-x} &= (u_{i-1,j,k+1} - u_{i-1,j,k-1})/2 \\
D_z^{+y} &= (u_{i,j+1,k+1} - u_{i,j+1,k-1})/2 & D_z^{-y} &= (u_{i,j-1,k+1} - u_{i,j-1,k-1})/2
\end{aligned} \tag{3.9}$$

Using the *difference of normals* method from [12], curvature is computed using the above derivates with the two normals $\mathbf{n}^+$ and $\mathbf{n}^-$.

$$\mathbf{n}^{+} = \begin{bmatrix} \frac{D_x^+}{\sqrt{(D_x^+)^2+\left(\frac{D_y^{+x}+D_y}{2}\right)^2+\left(\frac{D_z^{+x}+D_z}{2}\right)^2}} \\ \frac{D_y^+}{\sqrt{(D_y^+)^2+\left(\frac{D_x^{+y}+D_x}{2}\right)^2+\left(\frac{D_z^{+y}+D_z}{2}\right)^2}} \\ \frac{D_z^+}{\sqrt{(D_z^+)^2+\left(\frac{D_y^{+z}+D_x}{2}\right)^2+\left(\frac{D_y^{+z}+D_y}{2}\right)^2}} \end{bmatrix} \tag{3.10}$$

$$\mathbf{n}^{-} = \begin{bmatrix} \frac{D_x^-}{\sqrt{(D_x^-)^2+\left(\frac{D_y^{-x}+D_y}{2}\right)^2+\left(\frac{D_z^{-x}+D_z}{2}\right)^2}} \\ \frac{D_y^-}{\sqrt{(D_y^-)^2+\left(\frac{D_x^{-y}+D_x}{2}\right)^2+\left(\frac{D_z^{-y}+D_z}{2}\right)^2}} \\ \frac{D_z^-}{\sqrt{(D_z^-)^2+\left(\frac{D_y^{-z}+D_x}{2}\right)^2+\left(\frac{D_y^{-z}+D_y}{2}\right)^2}} \end{bmatrix} \tag{3.11}$$

The two normals are used to compute divergence, allowing for mean curvature to be computed as shown below in equation (3.12).

$$H = \frac{1}{2}\nabla \cdot \frac{\nabla\phi}{|\nabla\phi|} = \frac{1}{2}((\mathbf{n}_x^+ - \mathbf{n}_x^-) + (\mathbf{n}_y^+ - \mathbf{n}_y^-) + (\mathbf{n}_z^+ - \mathbf{n}_z^-)) \tag{3.12}$$

3.1.3 Stability

From [17], a finite difference approximation to a linear partial differential equation is convergent if and only if it is both consistent and stable. Stability implies that small errors in the solution are not amplified during iteration. Stability is enforced using the Courant-Friedreichs-Lewy (CFL) condition which states the numerical wave speed must be greater than the physical wave speed, i.e. $\Delta x/\Delta t > |u|$. Rearranging, we have

$$\Delta t < \frac{\Delta x}{max\,\{|u|\}} \tag{3.13}$$

which is usually implemented, through variants of equation (3.13), by choosing a *CFL number* that lies between 0 and 1 to further guarantee stability.

Another measure taken to ensure stability is the inclusion of a floating point relative accuracy term in the denominator of any fractions to avoid singularity errors as the denominator tends

to zero. This is done in equations (3.10),(3.11) to ensure that **n** does not tend to infinity if the square root is zero.

3.2 Sequential Implementation

Two dimensional implementations of the code in MATLAB, C and then CUDA were the first to be written. Once these had been optimized, three dimensional implementations were coded. The following pseudocode outlines the structure of the MATLAB, C and CUDA implementations, with only minor differences between the different versions.

Algorithm 1: Pseudocode for Level Set Segmentation

Input: Feature Image I, Initial Mask m, Threshold T, Range ϵ, Iterations N
Output: Segmentation Result

Initialise ϕ_0 to S.D.F from mask m
Calculate Data Speed Term $D(I) = \epsilon - |I - T|$
forall N *Iterations* **do**
  Calculate First Order Derivatives $D_x^{(\pm)}, D_y^{(\pm)}, D_z^{(\pm)}$
  Calculate Second Order Derivatives $D_x^{(\pm y,z)}, D_y^{(\pm x,z)} ... D_z^{(\pm x,y)}$
  Calculate Curvature Terms $\mathbf{n}^+, \mathbf{n}^-$
  Calculate Gradient $\nabla\phi$
  Calculate Speed Term $F = \alpha D(\bar{x}) + (1-\alpha)\nabla \cdot \frac{\nabla\phi}{|\nabla\phi|}$
  Update Level Set Function $\phi(t + \Delta t) = \phi(t) + \Delta t F|\nabla\phi|$
  if *Iterations % 50 == 0* **then**
    Reinitialise ϕ to S.D.F
  end
end

3.2.1 Matlab

The first task was to write code in MATLAB to learn about the inner workings of 2D image segmentation. The MATLAB Image Processing Toolbox provides many functions (such as the ability to load, resample and filter images, compute distance transforms and easily visualise the level set evolution) which kept code reasonably concise.

The code is split into two files (a launcher and a kernel), in order to seperate the initialisation and level set update code. The launcher handles the image loading and resampling, with the functions `imread` and `imresize`. The user specifies parameters for threshold values T, range ϵ and curvature weighting α, runs the launcher and then proceeds to draw a closed polygon that

will form the initial mask (providing some basic interactivity).

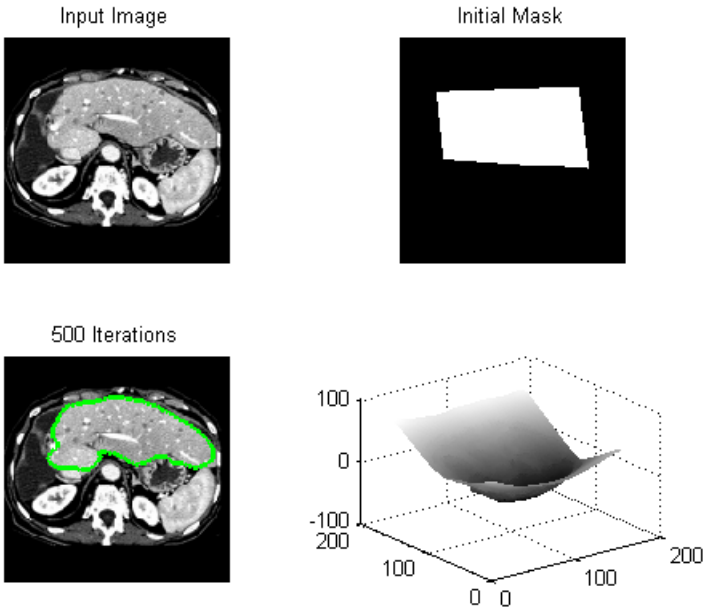

Figure 3.1: MATLAB user interface showing four subfigures with the input image, the initial mask, the current zero level set interface superimposed on the input image and the current level set surface in 3D

The level set function ϕ is then initialised to a signed distance function of this mask, and iteration of the level set equation begins for a fixed number of iterations (also user-definable). Reinitialisation of the level set is performed once every 50 iterations, and the current level set contour and surface are displayed every 20 iterations.

The derivatives are calculated by subtracting shifted matrices of ϕ from ϕ (or vice-versa). Note how derivatives are not calculated in an element by element fashion.

The MATLAB code also features the Courant-Friedreichs-Lewy (CFL) condition which was described in section 3.1.3 to enforce stability, instead of arbitrarily defining Δt.

Finally, the user has the option of downsampling the input image in order to speed up the computation.

The MATLAB code was later adapted to 3D volume segmentation.

3.2.2 C

Initially C code was written to most closely mirror the MATLAB code. The C code would serve as check for the parallel implementations to ensure correct values were calculated, the *gold*

version. The feature image, level set function, and derivatives were stored in memory as one dimensional arrays. These arrays were stepped through by nested for loops, looping i looping j. To go from the two dimensional i, j indices to a one dimensional index *ind*, the equation ind $= j \times$ imageW $+ i$ was used. These for loops computed the derivatives serially, as shown in the pseudocode for algorithm 2. This approach favoured itself well to being optimized at a low level using pointers to quickly step through the data. It was inefficient from a memory management perspective, with the derivative arrays taking up large amounts of memory for large image sizes, and also continuously being allocated and freed at each iteration.

Algorithm 2: Pseudocode for Version 1 of Sequential C Code

forall i, j **do**
  Calculate D_x
forall i, j **do**
  Calculate D_y
forall i, j **do**
  Calculate D_z
forall i, j **do**
  Calculate D_x^+
...
Update Level Set Function $\phi(t + \Delta t) = \phi(t) + \Delta t F |\nabla \phi|$

This C implementation did not feature the versatility of the MATLAB implementation as it only accepted bitmap images as the input for the feature image. The loader function for the bitmap images (`bmploader.cpp`) is from the NVIDIA CUDA SDK image processing examples. It also did not feature any image resizing functions, as the focus was on speed of the code and not versatility of inputs.

Wheras the MATLAB code used shifts of the matrix ϕ to calculate derivatives, in C the level set function ϕ was being stepped through in an element by element fashion. Therefore many boundary conditions had to be placed in order to ensure that derivatives took the value zero at certain boundaries. For example the forward difference derivative $D_x^+ = u_{i+1,j} - u_{i,j}$ must equal zero when $i =$ imageW as there is no $u_{i+1,j}$ term. The complexity of this task increases in three dimensions as there are six boundaries instead of four boundaries to condition for.

Restructuring the code for parallel computation of derivatives (using only one for loop) laid the framework for parallelization in CUDA, and only had a minor impact on performance. In this case all the derivatives are calculated at the same time at a given pixel, as shown below in

algorithm 3. Also, the derivatives no longer needed to be stored in memory as arrays, and were simply floating point variables declared at each iteration. These two changes condensed the C code greatly.

Algorithm 3: Pseudocode for Version 2 of Sequential C Code

forall i, j **do**
    Calculate D_x
    Calculate D_y
    Calculate D_z
    Calculate D_x^+
    ...
Update Level Set Function $\phi(t + \Delta t) = \phi(t) + \Delta t F |\nabla \phi|$

For the distance transform initialization and reinitialization procedures a seperate function was called. This is the `sedt2d` (Signed Euclidean Distance Transform in 2D) function written by Timothy Terriberry.

In order to visualise the level set evolution the combination of OpenGL and GLUT (OpenGL Utility Toolkit) was used to render the current zero level set. Rendering code was kept as compact and efficient as possible in order to have as minimal an effect as possible on performance whilst also making the program more comparable with the MATLAB code. Its principal purpose was of course to visualise how the level set was evolving (checking for instabilities, incorrect parameters for thresholding, range and curvature) and also view the final segmentation.

3.3 Parallel Implemention

3.3.1 Unoptimized Version

The first parallel implementation followed the structure shown in the pseudocode below. In CUDA, it is assumed that both the host and device maintain their own DRAM [15]. Host memory is allocated as before using `malloc` and device memory is allocated using `cudaMalloc`. As memory bandwidth between the host memory and device memory is low (it is much lower than the bandwidth between the device and the device memory), it is recommended to keep the number of transfers to a minimum. In order to minimise the latency of accessing the shared memory it is recommended to make the block size a multiple of 16 and use the `cudaMallocPitch` routine to allocate memory with padding if the images's x dimension is not a multiple of 16.

Therefore most CUDA programs follow a standard structure of initialization, host to device data transfer, compute, and finally memory transfer of compute results from device to host.

Unfortunately the algorithm for computing signed distance transforms is not executed in CUDA and creating one from scratch would have been beyond the scope of this project. Therefore device to host memory transfers were required every time reinitialization was necessary. Of course, when timing it is possible to stop and start timers during this process.

Algorithm 4: Parallel Implementation Pseudocode

Initialise $\phi_{i,j}^{(}0), D$ on host memory
Allocate memory for ϕ_n, ϕ_{n+1}, D on device
Copy ϕ_0, D from host to device
forall *N Iterations* **do**
  Execute Level Set Update CUDA Kernel $\phi_{i,j}^{(}n+1) = \phi_{i,j}^{(}n) + \Delta t F|\nabla\phi_n|$
  Swap pointers of $\phi_{i,j}^{(}n), \phi_{i,j}^{(}n+1)$
  if *Iterations % 50 == 0* **then**
    Copy ϕ from device to host
    Reinitialise ϕ to S.D.F
    Copy ϕ from host to device
  end
end
Copy ϕ from device to host

CUDA threads are assigned a unique thread ID that identifies its location within the thread-block and grid. This provides a natural way to invoke computation across the image and level set domain, by using the thread IDs for addressing. This is best explained with the tables below. Assume our image has dimensions 4×4 and the block size is 2×2. Invoking the kernel with a grid size of 2 blocks $\times$ 2 blocks results in the 16 threads shown in table 3.3.1, in the form (`threadIdx.y`,`threadIdx.x`). These threads are grouped into blocks of four, as shown in table 3.3.1, in the form (`blockIdx.y`,`blockIdx.x`).

As each thread has access to its own `threadIdx` and `blockIdx`, global indices (i, j) can be determined using the equations

(0,0)	(0,1)	(0,1)	(0,1)
(1,0)	(1,1)	(1,0)	(1,1)
(0,0)	(0,1)	(0,0)	(0,1)
(1,0)	(1,1)	(1,0)	(1,1)

Table 3.1: Thread IDs of 16 threads grouped into 4 blocks

(0,0)	(0,1)
(1,0)	(1,1)

Table 3.2: Block IDs of 4 blocks grouped into a grid

```
int i = blockIdx.x * blockDim.x + threadIdx.x;
int j = blockIdx.y * blockDim.y + threadIdx.y;
```

where `blockDim.x` and `blockDim.y` represent the dimensions of the block (which in this case are both equal to 2). Of course, much larger block sizes are used, keeping the block x dimension (BX) a multiple of 16 for maximum speed. The effect of different block sizes on performance is analysed in Section 4.1.2.

Once these indices were set up, it was relatively straightforward to transfer the level set update code to a CUDA kernel. Although this code exhibited speedups over the single threaded implementation, there was still significant optimization to perform as a great deal of computation time was being wasted on access global memory continuously. Therefore this is a *naive* implementation.

Some features such as the CFL condition, could not be implemented in this parallel version without slowing down computation time significantly. This is because such a condition requires the determination of the largest element of $\nabla\phi$ which is computed roughly half way through the update procedure. Therefore integrating this condition would require transferring $\nabla\phi$ and curvature terms back to host memory to determine $max\{F|\nabla\phi|\}$, or perhaps more efficiently calling a CUDA kernel to determine the largest element. The cost of this added complexity and slowdown outweighed the benefits, and therefore Δt was chosen to be a free parameter.

3.3.2 2D Shared Memory Optimization

In order to keep the number of costly accesses to device memory at a minimum, effective use of the on-chip shared memory is essential. This along with maximizing parallel execution and optimization of instruction usage form the three main performance optimization strategies for CUDA [15].

Integrating use of the shared memory into the CUDA kernel requires partitioning the level set domain into tiles. For first order finite difference problems such as ours each tile must also contain values for neighbourhood nodes (often known as *halo* nodes) for the $i \pm 1$ and $j \pm 1$

elements, which would be stored in seperate tiles, so these must also be read into shared memory. As the size of the shared memory is only 16 KB, the sizes of the tiles and corresponding halo are limited. [13] outlines a framework for such a process that may serve as a good model for a multi GPU implementation, however the kernel will need to be modified as it is optimized for higher order stencils (without cross-derivative terms). Instead, tiling code was adapted from Giles' (2008) 'Jacobi iteration for Laplace discretisation' algorithm [6] which supports cross-derivatives well. The shared memory management technique in this finite difference algorithm accelerated the global memory implementation by over an order of magnitude.

The two dimensional segmentation algorithm does not require any $k \pm 1$ terms, making the shared memory management more straightforward. For a block (and tile) size of $BX \times BY$ there are $2 \times (BX + BY + 2)$ halo elements, as can be seen in Figure 3.2. In this figure the darker elements represent the thread block (the active tile) and the lighter elements represent the halo. It is in this manner that the domain of the computation is partitioned and this results in overlapping of the halo nodes.

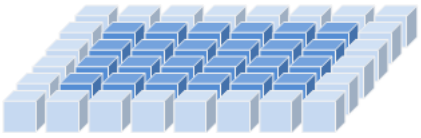

Figure 3.2: 2D Shared Memory Arrangement

Each thread loads ϕ_n values from global memory to the active tile stored in shared memory. However, depending on the location of the thread within the thread block it may also load a single halo node into the shared memory. Therefore in order to load all halo nodes, this technique assumes that there are at least as many interior nodes as there are halo nodes. Before data can be loaded into the halos, the thread ID needs to be mapped to the location of a halo node both within the halo and within the global indices. The segment of code that sets up the halo indices (both local and global) for loading into shared memory is shown below, code is from [6].

```
k    = threadIdx.x + threadIdx.y*BLOCK_X;
  halo = k < 2*(BLOCK_X+BLOCK_Y+2);

  if (halo) {
    if (threadIdx.y<2) {                // y-halos (coalesced)
      i = threadIdx.x;
```

```
  j = threadIdx.y*(BLOCK_Y+1) - 1;
}
else {                              // x-halos (not coalesced)
  i = (k%2)*(BLOCK_X+1) - 1;
  j =  k/2 - BLOCK_X - 1;
}
```

The first $2 \times (BX + BY + 2)$ threads are assigned to load values into the halo in this manner. This is best visualised with the example of a 6×6 thread block as shown below in Figure 3.3.

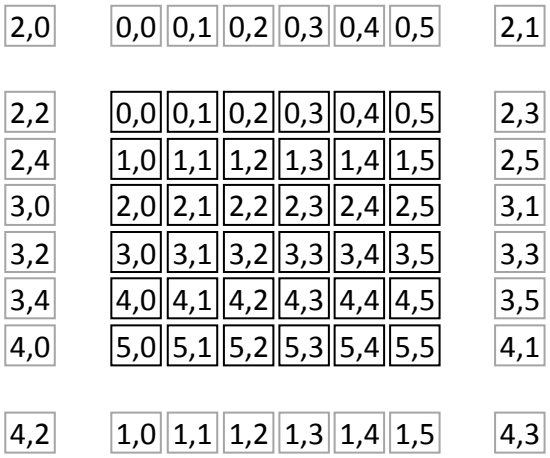

Figure 3.3: Tile and halo showing for a 6×6 block the mapping of thread IDs to halo nodes

This method of loading elements has been chosen in order to maximise *coalescence*. Not only are the interior tile nodes loaded coalesced, but as can be seen above, the first 12 elements of the thread block load the y halos (above and below the the interior tile excluding corners) in a coalesced manner. The side halos (x halos) loads are non-coalesced. When writing back results to global memory, as only the interior nodes have updated values they are written to global memory coalesced.

3.3.3 3D Shared Memory Optimization

In three dimensions, $k \pm 1$ terms are required and therefore these values need to also be stored in shared memory. CUDA only allows for two dimensional grid sizes (even though blocks can be three dimensional), implying that the number of blocks in the z dimension cannot exceed 1.

The algorithm by Giles [6] uses three k-planes of data for this purpose as shown in Figure

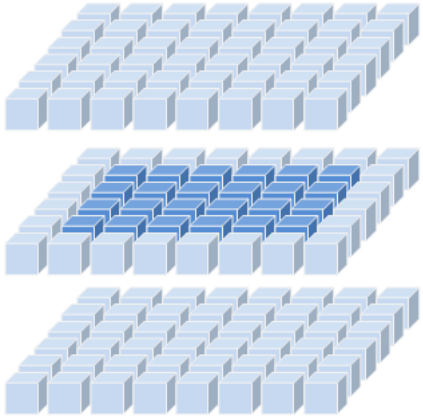

Figure 3.4: 3D Shared Memory Arrangement

3.4.

Before looping over the k-planes begins, the ϕ_k plane is loaded into the $k+1$ plane of shared memory. Upon entering the loop this plane is shifted down one plane to the k plane and the ϕ^n_{k+1} plane is loaded into the $k+1$ plane. Level set function values for ϕ^{n+1}_k are calculated and written coalesced back to global memory. The k plane is then shifted to the $k-1$ plane, the $k+1$ plane is shifted to the k plane, and new values are loaded from ϕ^n_{k+1} to the $k+1$ plane. This looping over the z dimension continues for all $z <$ imageD. In this manner, each block actually processes a $BX \times BY \times$ imageD sub domain.

Chapter 4

Results

In the following, the results of the speed ups attained by optimizing using CUDA will be shown. However, before this can be done, some preliminaries need to be listed. Firstly, all hardware testing was done on a single PC with an Intel Core 2 Duo T8100 Processor with a clock speed of 2.1 GHz and 4 GB of RAM. The graphics hardware used was the NVIDIA GeForce 8600M GT, with CUDA 2.1 software installed. It should be noted that at the time of writing, CUDA 2.2 was available although in beta form and was not chosen due to potential instabilities. Timing code used was from the `cutil` library.

Although 8600M GT is adequate for CUDA development, it has rather limited performance in comparison to other graphics chips. This implies that the performance speed ups below could potentially be up to a further order of magnitude faster on newer hardware. For example, although the shader processing rate of 8600M GT is quoted as 91.2 Gigaflops the recently released GeForce GTX 295 boasts an impressive 1788.48 Gigaflops potentially allowing for another order of magnitude speed up from the 8600M GT hardware. This is mainly due to the increased number of on chip multiprocessors, however to lesser extent is also due to the device being of higher *compute capability*: there are fewer limitations (such as support for double precision arithmetic) and relaxed requirements for coalescing memory transfers.

4.1 Speed Tests and Analysis

4.1.1 2D Segmentations

In Figure 4.1 the example of a liver segmentation is shown. The liver data is of good contrast and dimension 256×256 (which is a multiple of 16 implying no memory padding is required in CUDA). The liver has been entirely segmented, with the initial mask as the input. The time taken for 5000 iterations in MATLAB, C, CUDA (Unoptimized) and CUDA (Optimzed) are shown in Table 4.1.

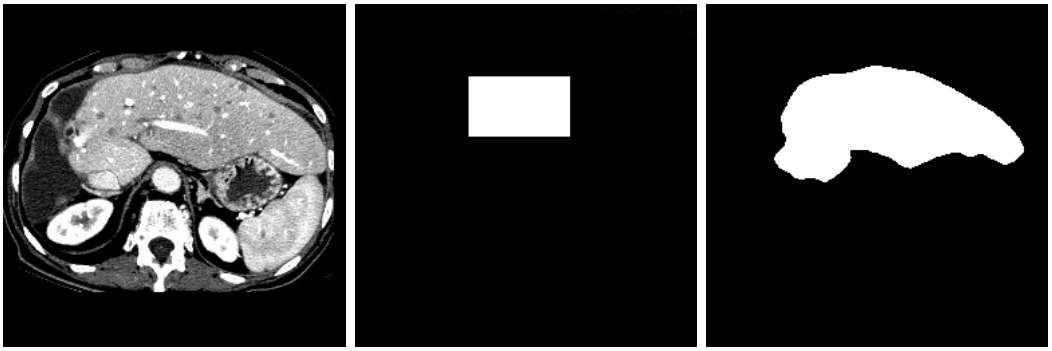

(a) Feature Image Input - Liver (b) Initial Mask Input (c) Output of Segmentation

Figure 4.1: 2D Liver Segmentation with parameters $T = 180, \epsilon = 45, \alpha = 0.003$

Algorithm Version	Time (s)
MATLAB	425.95
C	55.44
CUDA (Unoptimized)	8.38
CUDA (Optimized)	1.73

Table 4.1: Comparison of runtime for different algorithm versions - 2D liver segmentation

The runtime speed up attained from sequential code in C to CUDA optimized code is approximately $32\times$. The block sizes used for 2D CUDA compute were 32×8 (the effect of varying block sizes in 3D is examined in 4.1.2.

In Figure 4.2 we can see the brain in sagittal view. This image is of relatively poor contrast and has dimensions 512×512. This makes the image both a computationally demanding segmentation (as it has relatively large dimensions) and challenging in terms of accuracy. The segmentation inputs and output can be seen in Figure 4.2. It can be seen that the sequential algorithm has perfomed reasonably in segmenting the white and grey matter and some of the brian stem. Considerable weighting had to be given to curvature in order to prevent leaks due

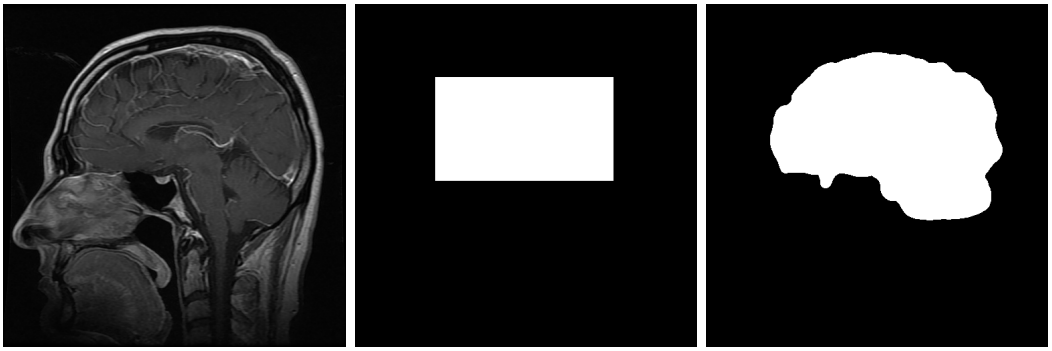

(a) Feature Image Input - brain (b) Initial Mask Input (c) Output of Segmentation

Figure 4.2: 2D Brain Segmentation with parameters $T = 45, \epsilon = 30, \alpha = 0.003$

to the poor contrast, resulting in a very rounded segmentation.

Algorithm Version	Time (s)
MATLAB	2737.84
C	322.81
CUDA (Unoptimized)	44.68
CUDA (Optimized)	6.99

Table 4.2: Comparison of runtime for different algorithm versions - 2D brain segmentation

The performance speedup attained on this larger image is therefore 46×, which is greater than the speed up attained for the smaller 256×256 image. This motivates exploration into the effect of different image sizes on CUDA speed up, which is discussed in Section 4.1.1.

Effect of Noise

Denoising filters already exist as part of the CUDA SDK (i.e. `imageDenoising`). Our algorithm does not feature any image pre-processing algorithms such as denoising or blurring so its performance on noisy images is expected to be poor. In order to test this, artificial noise of 20% and 40% was added to the liver image as shown in Figure 4.3.

It can be seen that through manipulating the parameter ϵ segmentations are still approximately valid. The effect of noise on performance of the algorithm was negligable.

Effect of Different Image Sizes

It is found, as expected, that for all versions of the algorithm (CUDA and single threaded) compute time scales proportionally with the number of elements. For square 2D images, this

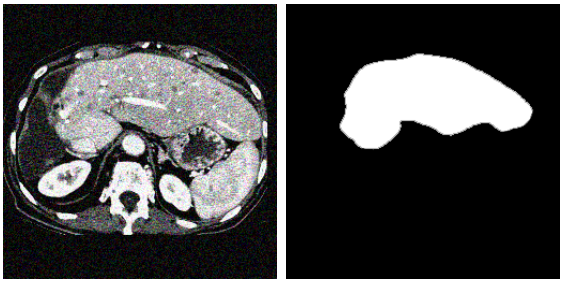

(a) Liver with 20% Noise

(b) Segmentation with $T = 180, \epsilon = 55, \alpha = 0.003$

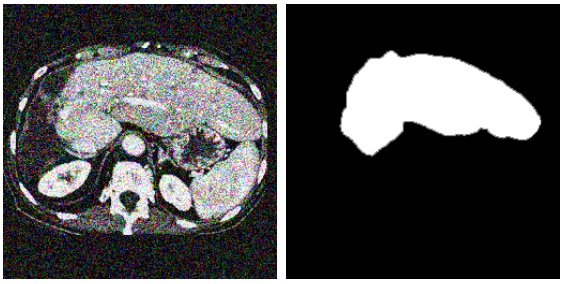

(c) Liver with 40% Noise

(d) Segmentation with $T = 180, \epsilon = 75, \alpha = 0.003$

Figure 4.3: Segmentation of the liver with artifically added noise

implies that increasing image size by a factor of two in each dimension increases compute time by a factor of four. Figure 4.4(a) displays compute times to 5000 iterations across the different algorithm versions. The same input image and mask was used for all test, with block dimensions of 32×8.

It can be seen that the difference in compute time between the parallel and sequential versions is greatest for the largest images. This is due to the number of elements for the optimized CUDA version being considerably higher for all image sizes. Interestingly, Figure 4.4(b) shows that the number of elements computed per second is approximately constant for both the sequential and unoptimized CUDA implementations, but not for the optimized shared memory CUDA algorithm. This is due to the bottleneck being latency between device and shared memory and there not being enough occupancy of the GPU to mask this.

4.1.2 3D Segmentations

Figure 4.5 illustrates a level set surface evolving in 3 dimensions. In order to visualise the level set evolving every certain number of iterations this the CUDA SDK example `volumeRender`

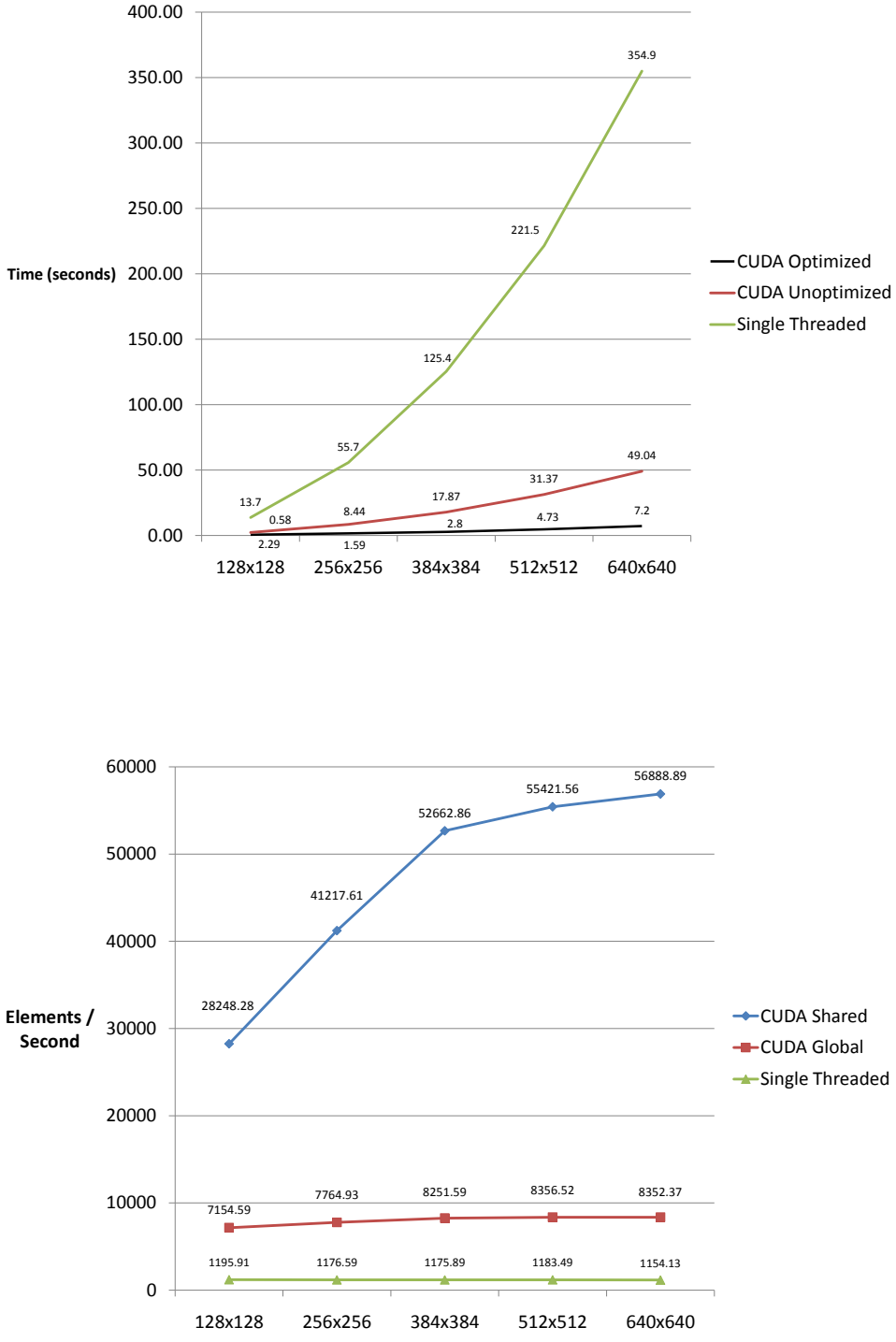

Figure 4.4: Effect of different image sizes (a) On compute time (b) On number of elements computed per second]

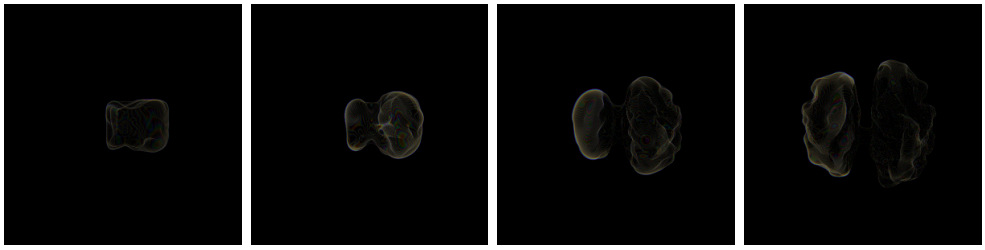

Figure 4.5: Level Set Surface Evolution in 3D at 50, 200, 400 and 600 Iterations

was modified, however is not advised as doing so slows down the segmentation process by approximately an order of magnitude. This volume rendering engine uses ray tracing which is not advised for segmentation inspection, and therefore *Paraview 3.4.0* (www.paraview.org) was used.

The 3D segmentation CUDA code uses a block size of 32×4. A block size of 32×8 causes the kernel invokation to fail due to the registers used per threads multiplied by the thread block size being greater N (where for G80 NVIDIA hardware $N = 8192$ 32-bit registers per multiprocessor. This limits the extent to which occupancy can be increased to mask latencies due to global memory loads. Section 4.1.2 explores the effect of varying block sizes on performance.

As can be seen in Figure 4.6 segmentation of the grey and white matter along with the brain stem is very anatomically detailed. This is due in part to the excellent quality of the *BrainWeb* MRI data used (data is available from [4]). As the CFL condition had not been implemented in the 3D level set solver, it was found to converge at 1000 iterations and that DT values greater than 0.1 resulted in instability.

The times taken to segment are shown in Figure 4.3. MATLAB code is not shown as out of memory errors were encountered when loading such large arrays (even if these had not been encountered, the segmentation would have taken an infeasible amount of time).

Algorithm Version	Time (s)
MATLAB	N/A
C	4697.5
CUDA (Unoptimized)	392.8
CUDA (Optimized)	141.2

Table 4.3: Comparison of runtime for different algorithm versions - 3D Brain segmentation

An impressive speed up of 33× is observed. To further demonstrate the power of this algorithm testing was briefly done on a more mid-range 8800 GTX card, observing a speed up

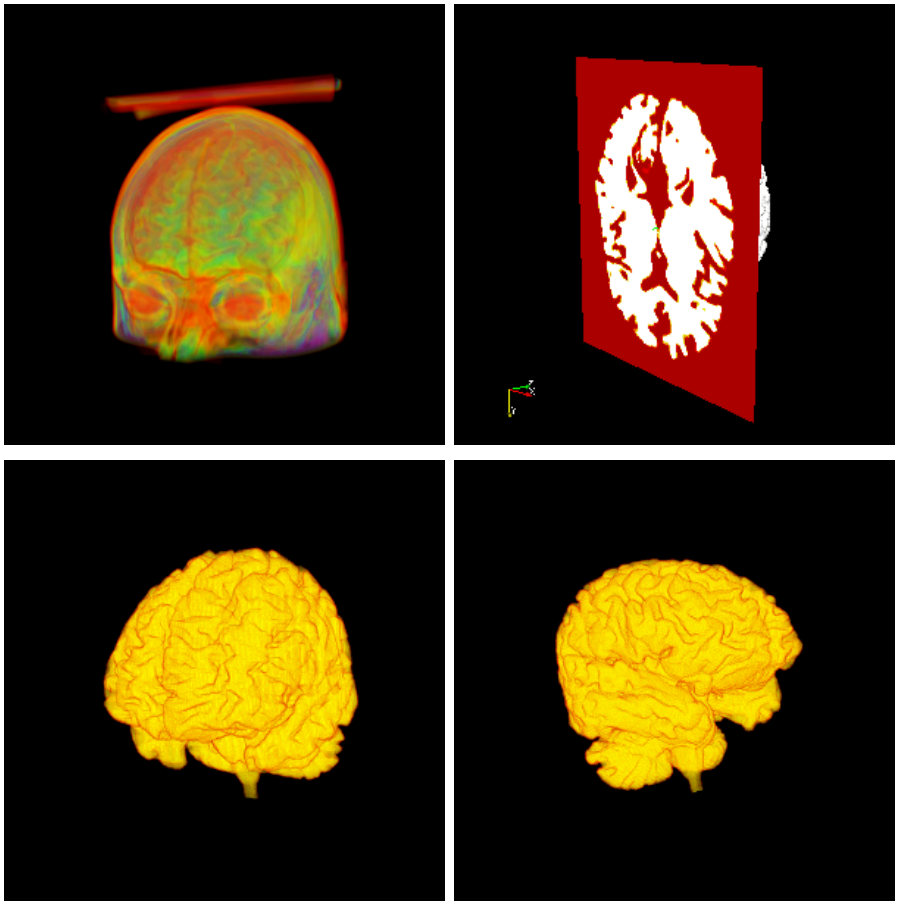

Figure 4.6: Segmentation of a brain MRI dataset with parameters $T = 150, \epsilon = 50, \alpha = 0.03$ MRI data from [4]

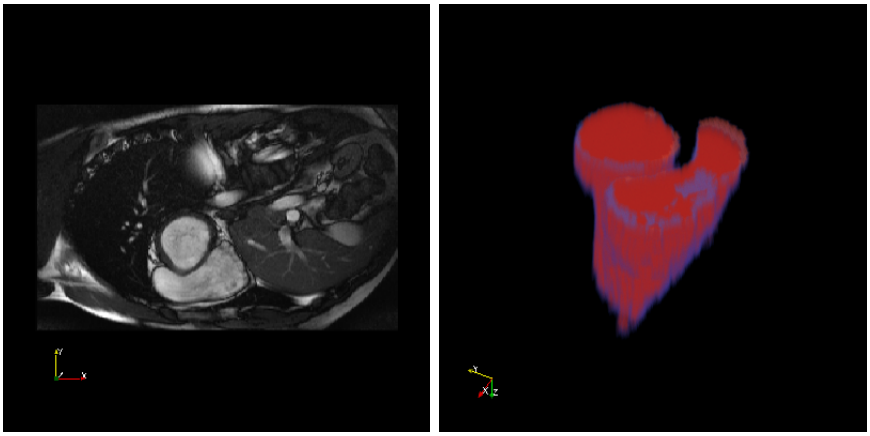

(a) (b)

Figure 4.7: Segmentation of the right and left ventricles from a heart MRI dataset with parameters $T = 180, \epsilon = 60, \alpha = 0.02$ (a) Input data slice (b) Segmented heart clipped through z plane

of 117× compared to the sequential algorithm.

In Figure 4.7 segmentation of both the right and left ventricles can be seen. This segmentation data only had 17 z plane slices (total resolution $256 \times 160 \times 17$).

Effect of Different Volume Sizes

Table 4.4 shows the effect of multiple volume sizes on the compute time to 1000 iterations on the optimized CUDA algorithm. Tests were not run on unoptimized or sequential code as results similar to those in As the CUDA optimized algorithm loops over the k planes in a sequentially fashion, it is expected that doubling the volume size in the z dimension would have an effect on compute time when compared to doubling the volume sizes in either the x or y dimensions. Therefore testing was done on non-cubic volume dimensions in order to explore this effect.

Volume Dimensions	Elements / Second	Time (s)
$64 \times 64 \times 64$	54050.3	4.9
$128 \times 128 \times 128$	53676.8	39.1
$128 \times 256 \times 128$	53092.5	79.0
$128 \times 128 \times 256$	53485.1	78.4
$256 \times 256 \times 256$	52925.0	317.1

Table 4.4: Comparison of runtime for different volume sizes

In fact, it is found that there is no effect on performance which demonstrates the algorithms versatility.

Effect of Different CUDA Block/Grid Sizes

Finding the optimum block size for CUDA code is one of the most important ways to optimize performance. Block sizes should not be a user parameter (other than for testing purposes) as it assumed the developer would have chosen the optimum block size for maximum performance. Figure 4.5 shows the compute times to 1000 iterations for the CUDA optimized code with different block sizes, all other parameters were held constant.

It can be seen that for blocks with 192 threads performance is approximately constant across the different block arrangements. This is due to the fact that BX has been chosen to be a multiple of 16 to maximise performance, the parameter BY has much less of an effect on performance and should always be set secondary to BX.

$BX \times BY$	Threads/Block	Time (s)
32×4	128	141.7
16×8	128	141.9
16×12	192	108.4
32×6	192	107.4
48×4	192	106.8

Table 4.5: Comparison of runtime for different block sizes

4.2 Discussion and Limitations

4.2.1 Speed

This algorithm does not currently use a narrow band, introduced in Section 3.1.1, to update the level set in either the sequential or parallel versions, making the algorithm more of a 'brute force' approach to segmentation. This is a feature to be included in the next version of the algorithm and has potential to further speed the algorithm by another order of magnitude.

Comparison of CPU and GPU code was done with algorithms that most closely mirrored each other. Although this standardizes the code, it does distort the results slightly as there is potential for optimizaton on the CPU by making effective use of the CPU cache, and multiple cores (if present).

Goodman [7] shows that CPU code may be slowed if a GPU kernel is executed and therefore suggests that CPU and GPU code run in seperate independent environments. To this effect, this has been catered for, increasing the accuracy of the speed up figures attained.

Furthermore, making comparisons with MATLAB code is inadvisable given the environment that MATLAB code runs. MATLAB code is JIT compiled, creating many problems when directly comparing compute times between the two versions. Speed ups were for this reason not measured against MATLAB code. In fact, the main purpose of the MATLAB code was to learn about the inner workings of level set segmentation.

4.2.2 Accuracy

The nature of segmenting images using thresholding and curvature terms favours segmentations of anatomical objects with a relatively homogenous gray value range. As the focus was on speed, a great deal of testing was not done on these forms of images.

Secondly, as discussed in Section 2.2.2 the current 3D level set segmentation solver does not

integrate a reinitialisation algorithm. This is the largest limitation of this algorithm as it may result in instabilities in the level set function if $\nabla\phi$ values get too large. It should be noted that when implementing a 3D distance transform there is a major trade off between accuracy and speed.

Finally, there are currently no built in preprocessing filters. Denoising, blurring, sharpening and edge detection would most likely produce more accurate segmentations without affecting performance too greatly (provided CUDA kernels are used for these filters).

Chapter 5

Conclusions and Future Work

5.1 Conclusion

In this project report a fast segmentation algorithm has been presented and analysed. The implementation on the graphics device is very fast, with large two dimensional images and three dimensional volumes segmented 30 to 40 times faster (on a relatively low performance GPU) than sequential algorithms. The method of using level sets to segment images, and how to accelerate this process using GPUs has been discussed in great detail. The numerical methods used for the implementation were listed in Section 3.1. Giles' CUDA kernel for laplace discretization in 3D [6] has been adapted for level set iteration. In Section 4.1 it was seen that the power of GPU acceleration was demonstrated for very large data sets.

Given the wide range of applications level sets have in computing (image processing, computer graphics and physical simulation) this algorithm serves as an excellent framework to solve a diverse array of problems.

CUDA itself has been shown to be an excellent framework to accelerate computational problems in engineering, and is gaining more features and fewer limitations every few months. The principal disadvantages of CUDA are that it is only effective for very data parallel problems, and that it is not an industry standard. Recently, to counter the latter, it is very likely that it will in fact be replaced by *OpenCL* (Open Computing Language). The syntax and architecture between CUDA and OpenCL will be very similar, allowing this code to be easily ported to OpenCL.

5.2 Future Work

There are several areas in which this algorithm could be improved which revolve around three central themes of speed, accuracy and usability.

In terms of speed, integrating the narrow band method into the algorithm will provide significant further speed up, however increases the complexity of the kernel (potentially resulting in higher register usage and therefore less occupancy). Secondly, adding support for multiple GPUs and testing on very high performance hardware would be of significant interest.

Including a 3D signed Euclidean distance transform function is very important for volume segmentation. This would need to be implemented in CUDA in order to prevent costly transfers of data from the device to the host. To increase accuracy, integrating filters in CUDA to preprocess the medical data is strongly encouraged. Including more terms into the level set speed function (such as edge stopping functions) would allow the algorithm to segment unhomogenous gray valued regions.

Finally, in order to make the segmentation more interactive and versatile, it is suggested to include a graphical user interface allowing segmentation to be visualized and guided at the same time. In order to ensure visualization does not affect performance it is suggested to use two GPUs: one to process the level set and the other to render the level set evolution.

Bibliography

[1] David Adalsteinsson and James A. Sethian. A fast level set method for propagating interfaces. *Journal of Computational Physics*, 118:269–277, 1994.

[2] J.E. Cates, A.E. Lefohn, and R.T. Whitaker. GIST: an interactive, GPU-based level set segmentation tool for 3D medical images. *Medical Image Analysis*, 8(3):217–231, 2004.

[3] T.F. Chan and L.A. Vese. Active contours without edges. *IEEE Transactions on image processing*, 10(2):266–277, 2001.

[4] Chris A. Cocosco, Vasken Kollokian, Remi K.-S. Kwan, G. Bruce Pike, and Alan C. Evans. Brainweb: Online interface to a 3d mri simulated brain database. *NeuroImage*, 5:425, 1997.

[5] Kent Roger B. Fagerjord and Tatyana V. Lochehina. *GPGPU: Fast and easy Distance Field computation on GPU*. 2008.

[6] Mike Giles. Jacobi iteration for a laplace discretisation on a 3d structured grid. 2008.

[7] Daniel Goodman. Measuring speed ups on graphics cards. 2009.

[8] C.L.C.X.C. Gui and MD Fox. Level set evolution without re-initialization: a new variational formulation. In *IEEE Computer Society Conference on Computer Vision and Pattern Recognition, 2005. CVPR 2005*, volume 1, 2005.

[9] L. Ibanez, W. Schroeder, L. Ng, and J. Cates. The ITK Software Guide. Kitware, Inc.

[10] A. Kharlamov and V. Podlozhnyuk. Image Denoising.

[11] O. Klar. Interactive GPU-based Segmentation of Large Medical Volume Data with Level-Sets.

[12] Aaron E. Lefohn, Joe M. Kniss, Charles D. Hansen, and Ross T. Whitaker. A streaming narrow-band algorithm: Interactive computation and visualization of level sets. *IEEE Transactions on Visualization and Computer Graphics*, 10:422–433, 2004.

[13] Paulius Micikevicius. 3d finite difference computation on gpus using cuda. In *GPGPU-2: Proceedings of 2nd Workshop on General Purpose Processing on Graphics Processing Units*, pages 79–84, New York, NY, USA, 2009. ACM.

[14] H. Nguyen. GPU gems 3. 2007.

[15] NVIDIA. Compute Unified Device Architecture–Programming Guide, 2008.

[16] NVIDIA. Compute Unified Device Architecture–Reference Manual, 2008.

[17] S. Osher and R.P. Fedkiw. *Level set methods and dynamic implicit surfaces*. Springer, 2003.

[18] Stanley Osher and James A. Sethian. Fronts propagating with curvature dependent speed: algorithms based on hamilton-jacobi formulations. *Journal of Computational Physics*, 79:12–49, 1988.

[19] M. Rumpf and R. Strzodka. Level set segmentation in graphics hardware. In *Image Processing, 2001. Proceedings. 2001 International Conference on*, volume 3, 2001.

[20] J.A. Sethian et al. Level set methods and fast marching methods. *Journal of Computing and Information Technology*, 11(1):1–2, 2003.

[21] O. Sharma and F. Anton. CUDA based Level Set Method for 3D Reconstruction of Fishes from Large Acoustic Data. In *International Conference in Central Europe on Computer Graphics, Visualization and Computer Vision 17*.

[22] A. Sud, M.A. Otaduy, and D. Manocha. DiFi: Fast 3D distance field computation using graphics hardware. In *Computer Graphics Forum*, volume 23, pages 557–566. Blackwell Publishing, 2004.

[23] Ross T. Whitaker. A level-set approach to 3d reconstruction from range data. *Int. J. Comput. Vision*, 29(3):203–231, 1998.

Appendix A

MATLAB 2D Code

```
function seg = simpleseg(I,init_mask,max_its,E,T,alpha)

%-- Create a signed distance map (SDF) from mask
phi=bwdist(init_mask)-bwdist(1-init_mask)-.5;

%main loop
for its = 1:max_its

    D = E - abs(I - T);
    K = get_curvature(phi);
    F = -alpha*D + (1-alpha)*K;

    dxplus=shiftR(phi)-phi;
    dyplus=shiftU(phi)-phi;
    dxminus=phi-shiftL(phi);
    dyminus=phi-shiftD(phi);

    gradphimax_x = sqrt(max(dxplus,0).^2+max(-dxminus,0).^2);
    gradphimin_x = sqrt(min(dxplus,0).^2+min(-dxminus,0).^2);
    gradphimax_y = sqrt(max(dyplus,0).^2+max(-dyminus,0).^2);
    gradphimin_y = sqrt(min(dyplus,0).^2+min(-dyminus,0).^2);
    gradphimax = sqrt((gradphimax_x.^2)+(gradphimax_y.^2));
    gradphimin = sqrt((gradphimin_x.^2)+(gradphimin_y.^2));
    gradphi=(F>0).*(gradphimax) + (F<0).*(gradphimin);

    %stability CFL
    dt = .5/max(max(abs(F.*gradphi)));

    %evolve the curve
    phi = phi + dt.*(F).*gradphi;

    %reinitialise distance funciton every 50 iterations
    if(mod(its,50) == 0)
        phi=bwdist(phi<0)-bwdist(phi>0);
    end

    %intermediate output
```

```
    if(mod(its,20) == 0)
        showcontour(I,phi,its);
        subplot(2,2,4);  surf(phi); shading flat;
    end
end

%make mask from SDF
seg = phi<=0; %-- Get mask from levelset

%-- whole matrix derivatives
function shift = shiftD(M)
shift = shiftR(M')';

function shift = shiftL(M)
shift = [ M(:,2:size(M,2)) M(:,size(M,2)) ];

function shift = shiftR(M)
shift = [ M(:,1) M(:,1:size(M,2)-1) ];

function shift = shiftU(M)
shift = shiftL(M')';

function curvature=get_curvature(phi)
dx=(shiftR(phi)-shiftL(phi))/2;
dy=(shiftU(phi)-shiftD(phi))/2;
dxplus=shiftR(phi)-phi;
dyplus=shiftU(phi)-phi;
dxminus=phi-shiftL(phi);
dyminus=phi-shiftD(phi);
dxplusy =(shiftU(shiftR(phi))-shiftU(shiftL(phi)))/2;
dyplusx =(shiftR(shiftU(phi))-shiftR(shiftD(phi)))/2;
dxminusy=(shiftD(shiftR(phi))-shiftD(shiftL(phi)))/2;
dyminusx=(shiftL(shiftU(phi))-shiftL(shiftD(phi)))/2;

nplusx = dxplus./sqrt(eps+(dxplus.^2 )+((dyplusx+dy )/2).^2);
nplusy = dyplus./sqrt(eps+(dyplus.^2 )+((dxplusy+dx )/2).^2);
nminusx= dxminus./sqrt(eps+(dxminus.^2)+((dyminusx+dy)/2).^2);
nminusy= dyminus./sqrt(eps+(dyminus.^2)+((dxminusy+dx)/2).^2);

curvature=((nplusx-nminusx)+(nplusy-nminusy)/2);

%-- Displays the image with curve superimposed
function showcontour(I, phi, i)
subplot(2,2,3); title('Evolution');
imshow(I,'initialmagnification',200,'displayrange',[0 255]);
hold on;
contour(phi, [0 0], 'g','LineWidth',2);
hold off; title([num2str(i) ' Iterations']); drawnow;
```

Appendix B

CUDA 3D Kernel Source Code

```
#define ALPHA              0.03
#define DT                 0.1

#define max(x,y)     ((x>y) ? x : y )
#define min(x,y)     ((x<y) ? x : y )

#define INDEX(i,j,j_off)  (i +__mul24(j,j_off))

#define BLOCKDIM_X         32
#define BLOCKDIM_Y         4
#define BLOCKDIM_Z         1

__global__ void updatephi( float *d_phi, float *d_phi1, float *d_D,
                int imageW, int imageH, int imageD, int pitch)
{

float dx,dy,dz;
float dxplus, dyplus, dzplus, dxminus, dyminus, dzminus;
float dxplusy, dxminusy, dxplusz, dxminusz, dyplusx, dyminusx,
        dyplusz, dyminusz, dzplusx, dzminusx, dzplusy, dzminusy;

float gradphimax, gradphimin;
float nplusx, nplusy, nplusz, nminusx, nminusy, nminusz, curvature;
float F, gradphi;

//M. GILES CUDA TILING CODE

int    indg, indg_h, indg0;
int    i, j, k, ind, ind_h, halo, active;

int IOFF  = 1;
int JOFF  = (BLOCKDIM_X+2);
int KOFF  = (BLOCKDIM_X+2)*(BLOCKDIM_Y+2);

__shared__ float s_data[3*(BLOCKDIM_X+2)*(BLOCKDIM_Y+2)];

k    =  threadIdx.y*BLOCKDIM_X + threadIdx.x;
```

```
halo = k < 2*(BLOCKDIM_X+BLOCKDIM_Y+2);

if (halo) {
        if (threadIdx.y<2) {                    // y-halos (coalesced)
                i = threadIdx.x;
                j = threadIdx.y*(BLOCKDIM_Y+1) - 1;
        }
        else {                                  // x-halos (not coalesced)
                i = (k%2)*(BLOCKDIM_X+1) - 1;
                j =  k/2 - BLOCKDIM_X - 1;
        }

        ind_h  = INDEX(i+1,j+1,BLOCKDIM_X+2)+KOFF;

        i      = INDEX(i,blockIdx.x,BLOCKDIM_X);    // global indices
        j      = INDEX(j,blockIdx.y,BLOCKDIM_Y);
        indg_h = INDEX(i,j,pitch);

        halo   =  (i>=0) && (i<imageW) && (j>=0) && (j<imageH);
}

//
// then set up indices for main block
//

i    = threadIdx.x;
j    = threadIdx.y;
ind  = INDEX(i+1,j+1,BLOCKDIM_X+2) ;

i    = INDEX(i,blockIdx.x,BLOCKDIM_X);      // global indices
j    = INDEX(j,blockIdx.y,BLOCKDIM_Y);
indg = INDEX(i,j,pitch);

active = (i<imageW) && (j<imageH);

//
// read initial plane of u1 array
//

if (active) s_data[ind+KOFF+KOFF] = d_phi1[indg];
if (halo) s_data[ind_h+KOFF+KOFF] = d_phi1[indg_h];


for(int k=0;k<imageD;k++){

if (active) {
        indg0 = indg;
        indg  = INDEX(indg,imageH,pitch);
        s_data[ind-KOFF] = s_data[ind];
        s_data[ind]      = s_data[ind+KOFF];
        if (k<imageD-1)
                s_data[ind+KOFF] = d_phi1[indg];
```

```
}

if (halo) {
        indg_h = INDEX(indg_h,imageH,pitch);
        s_data[ind_h-KOFF] = s_data[ind_h];
        s_data[ind_h]      = s_data[ind_h+KOFF];
        if (k<imageD-1)
                s_data[ind_h+KOFF] = d_phi1[indg_h];
}
//M. GILES CUDA TILING CODE END


if (active) {

if(i==0||i==imageW-1){dx=0;}
else {dx=(s_data[ind+IOFF]-s_data[ind-IOFF])/2;}
if(j==0||j==imageH-1){dy=0;}
else {dy=(s_data[ind-JOFF]-s_data[ind+JOFF])/2;}
if(k==0||k==imageD-1){dz=0;}
else {dz=(s_data[ind+KOFF]-s_data[ind-KOFF])/2;}

if(i==imageW-1){dxplus=0;}
else {dxplus =(s_data[ind+IOFF]-s_data[ind     ]);}
if(j==0){dyplus=0;}
else {dyplus =(s_data[ind-JOFF]-s_data[ind     ]);}
if(k==imageD-1){dzplus=0;}
else {dzplus =(s_data[ind+KOFF]-s_data[ind     ]);}
if(i==0){dxminus=0;}
else {dxminus=(s_data[ind     ]-s_data[ind-IOFF]);}
if(j==imageH-1){dyminus=0;}
else {dyminus=(s_data[ind     ]-s_data[ind+JOFF]);}
if(k==0){dzminus=0;}
else {dzminus=(s_data[ind     ]-s_data[ind-KOFF]);}

if(i==0||i==imageW-1||j==0){dxplusy=0;}
else {dxplusy =(s_data[ind-JOFF+IOFF]-s_data[ind-JOFF-IOFF])/2;}
if(i==0||i==imageW-1||j==imageH-1){dxminusy=0;}
else {dxminusy=(s_data[ind+JOFF+IOFF]-s_data[ind+JOFF-IOFF])/2;}
if(i==0||i==imageW-1||k==imageD-1) {dxplusz=0;}
else {dxplusz =(s_data[ind+KOFF+IOFF]-s_data[ind+KOFF-IOFF])/2;}
if(i==0||i==imageW-1||k==0) {dxminusz=0;}
else {dxminusz=(s_data[ind-KOFF+IOFF]-s_data[ind-KOFF-IOFF])/2;}
if(j==0||j==imageH-1||i==imageW-1){dyplusx=0;}
else {dyplusx =(s_data[ind-JOFF+IOFF]-s_data[ind+JOFF+IOFF])/2;}
if(j==0||j==imageH-1||i==0){dyminusx=0;}
else {dyminusx=(s_data[ind-JOFF-IOFF]-s_data[ind+JOFF-IOFF])/2;}
if(j==0||j==imageH-1||k==imageD-1) {dyplusz=0;}
else {dyplusz =(s_data[ind+KOFF-JOFF]-s_data[ind+KOFF+JOFF])/2;}
if(j==0||j==imageH-1||k==0) {dyminusz=0;}
else {dyminusz=(s_data[ind-KOFF-JOFF]-s_data[ind-KOFF+JOFF])/2;}
if(k==0||k==imageD-1||i==imageW-1) {dzplusx=0;}
else {dzplusx =(s_data[ind+IOFF+KOFF]-s_data[ind+IOFF-KOFF])/2;}
```

```
if(k==0||k==imageD-1||i==0) {dzminusx=0;}
else {dzminusx=(s_data[ind-IOFF+KOFF]-s_data[ind-IOFF-KOFF])/2;}
if(k==0||k==imageD-1||j==0) {dzplusy=0;}
else {dzplusy =(s_data[ind-JOFF+KOFF]-s_data[ind-JOFF-KOFF])/2;}
if(k==0||k==imageD-1||j==imageH-1) {dzminusy=0;}
else {dzminusy=(s_data[ind+JOFF+KOFF]-s_data[ind+JOFF-KOFF])/2;}


gradphimax=sqrt((sqrt(max(dxplus,0)*max(dxplus,0)+max(-dxminus,0)*max(-dxminus,0)))
        *(sqrt(max(dxplus,0)*max(dxplus,0)+max(-dxminus,0)*max(-dxminus,0)))
        +(sqrt(max(dyplus,0)*max(dyplus,0)+max(-dyminus,0)*max(-dyminus,0)))
        *(sqrt(max(dyplus,0)*max(dyplus,0)+max(-dyminus,0)*max(-dyminus,0)))
        +(sqrt(max(dzplus,0)*max(dzplus,0)+max(-dzminus,0)*max(-dzminus,0)))
        *(sqrt(max(dzplus,0)*max(dzplus,0)+max(-dzminus,0)*max(-dzminus,0))));

gradphimin=sqrt((sqrt(min(dxplus,0)*min(dxplus,0)+min(-dxminus,0)*min(-dxminus,0)))
        *(sqrt(min(dxplus,0)*min(dxplus,0)+min(-dxminus,0)*min(-dxminus,0)))
        +(sqrt(min(dyplus,0)*min(dyplus,0)+min(-dyminus,0)*min(-dyminus,0)))
        *(sqrt(min(dyplus,0)*min(dyplus,0)+min(-dyminus,0)*min(-dyminus,0)))
        +(sqrt(min(dzplus,0)*min(dzplus,0)+min(-dzminus,0)*min(-dzminus,0)))
        *(sqrt(min(dzplus,0)*min(dzplus,0)+min(-dzminus,0)*min(-dzminus,0))));

nplusx = dxplus / sqrt(1.192092896e-07F + (dxplus*dxplus)
        + ((dyplusx + dy)*(dyplusx + dy)*0.25)
        + ((dzplusx + dz)*(dzplusx + dz)*0.25));
nplusy = dyplus / sqrt(1.192092896e-07F + (dyplus*dyplus)
        + ((dxplusy + dx)*(dxplusy + dx)*0.25)
        + ((dzplusy + dz)*(dzplusy + dz)*0.25));
nplusz = dzplus / sqrt(1.192092896e-07F + (dzplus*dzplus)
        + ((dxplusz + dz)*(dxplusz + dz)*0.25)
        + ((dyplusz + dy)*(dyplusz + dy)*0.25));

nminusx=dxminus / sqrt(1.192092896e-07F + (dxminus*dxminus)
        + ((dyminusx + dy)*(dyminusx + dy)*0.25)
        + ((dzminusx + dz)*(dzminusx + dz)*0.25));
nminusy=dyminus / sqrt(1.192092896e-07F + (dyminus*dyminus)
        + ((dxminusy + dx)*(dxminusy + dx)*0.25)
        + ((dzminusy + dz)*(dzminusy + dz)*0.25));
nminusz=dzminus / sqrt(1.192092896e-07F + (dzminus*dzminus)
        + ((dxminusz + dz)*(dxminusz + dz)*0.25)
        + ((dyminusz + dy)*(dyminusz + dy)*0.25));

curvature = ((nplusx-nminusx)+(nplusy-nminusy)+(nplusz-nminusz))/2;

F = (-ALPHA * d_D[indg0]) + ((1-ALPHA) * curvature);
if(F>0) {gradphi=gradphimax;} else {gradphi=gradphimin;}
d_phi[indg0]=s_data[ind] + (DT * F * gradphi);

}
__syncthreads();
}
}
```

Appendix C

CUDA 3D Main Source Code

```
#include <stdio.h>
#include <stdlib.h>
#include <cuda_runtime.h>
#include <cutil.h>

#define BLOCKDIM_X      32
#define BLOCKDIM_Y      6
#define BLOCKDIM_Z      1

char *volumeFilename, *maskFilename;
int     ITERATIONS, THRESHOLD, EPSILON;
float alpha;
int imageW, imageH, imageD, N, pitch;

float *phi, *D;
size_t size, pitchbytes;
unsigned char *input,*output;

float *d_phi, *d_phi1, *d_D;

int its=0;
unsigned int Timer = 0;

int i,j,k;

__global__ void updatephi( float *d_phi, float *d_phi1, float *d_D,
        int imageW, int imageH, int imageD, float alpha, int pitch);

// loadRawUchar, loadMask, and writeoutput functions not of interest

void cuda_update(){

dim3 dimGrid( ((imageW-1)/BLOCKDIM_X) + 1, ((imageH-1)/BLOCKDIM_Y) +1);
dim3 dimBlock(BLOCKDIM_X, BLOCKDIM_Y, BLOCKDIM_Z);

updatephi<<< dimGrid, dimBlock>>>(d_phi, d_phi1, d_D,
        imageW, imageH, imageD, alpha, pitch);
```

```
d_phi1=d_phi;

CUT_CHECK_ERROR("Kernel execution failed\n");
CUDA_SAFE_CALL(cudaThreadSynchronize());
}

int main(int argc, char** argv){

// Ensure all parameters are set
if(argc<9){
        printf("Too few command line arguments specified\n");
        exit(0);
}

// Parse Command Line Arguments
cutGetCmdLineArgumentstr( argc, (const char**) argv, "volume", &volumeFilename);
cutGetCmdLineArgumentstr( argc, (const char**) argv, "mask", &maskFilename);
cutGetCmdLineArgumenti( argc, (const char**) argv, "xsize", &imageW);
cutGetCmdLineArgumenti( argc, (const char**) argv, "ysize", &imageH);
cutGetCmdLineArgumenti( argc, (const char**) argv, "zsize", &imageD);
cutGetCmdLineArgumenti( argc, (const char**) argv, "iterations", &ITERATIONS);
cutGetCmdLineArgumenti( argc, (const char**) argv, "threshold", &THRESHOLD);
cutGetCmdLineArgumenti( argc, (const char**) argv, "epsilon", &EPSILON);
cutGetCmdLineArgumentf( argc, (const char**) argv, "alpha", &alpha);

// Initialise Feature Image and Mask on Host
N=imageW*imageH*imageD;
input = loadRawUchar(volumeFilename, N);
phi = loadMask(maskFilename, N);

// Calculate D(I) = E - | I - T |
if((D = (float *)malloc(imageW*imageH*imageD*sizeof(float)))==NULL) printf("ME_D\n");
for(i=0;i<N;i++){
        D[i] = EPSILON - abs((unsigned char)input[i] - THRESHOLD);
}

// Set up CUDA Timer
cutCreateTimer(&Timer);

// Allocate Memory on Device
CUDA_SAFE_CALL( cudaMallocPitch((void**)&d_D, &pitchbytes,
        sizeof(float)*imageW, imageH*imageD));
CUDA_SAFE_CALL( cudaMallocPitch((void**)&d_phi,&pitchbytes,
        sizeof(float)*imageW, imageH*imageD));
CUDA_SAFE_CALL( cudaMallocPitch((void**)&d_phi1, &pitchbytes,
        sizeof(float)*imageW, imageH*imageD));

pitch=pitchbytes/sizeof(float);

// Copy Host Data to Device Memory
CUDA_SAFE_CALL( cudaMemcpy2D(d_D,pitchbytes, D, sizeof(float)*imageW,
        sizeof(float)*imageW, imageH*imageD, cudaMemcpyHostToDevice));
```

```
CUDA_SAFE_CALL( cudaMemcpy2D(d_phi1, pitchbytes, phi, sizeof(float)*imageW,
        sizeof(float)*imageW, imageH*imageD, cudaMemcpyHostToDevice));

// Start Timer
cutStartTimer(Timer);

// Iterate Level Set Solver
for(its=0;its<=ITERATIONS;its++){
        cuda_update();
        if(its%50==0){
        printf("Iteration %3d Time: %3.2f\n",
                its, 0.001*cutGetTimerValue(Timer),);}
}

// Stop Timer
cutStopTimer(Timer);

// Write Result Back to Host Memory
cudaMemcpy2D(phi, sizeof(float)*imageW, d_phi1, pitchbytes,

writeoutput(phi, N);

// Free Memory
CUDA_SAFE_CALL( cudaFree(d_phi) );
CUDA_SAFE_CALL( cudaFree(d_phi1) );
CUDA_SAFE_CALL( cudaFree(d_D) );
free(D);
free(phi);
free(input);

}
```

Full versions of all the above source code, and their revisions, can be seen at `cudaseg.googlecode.com`.

Department of Eng Science

4th Year Project Risk Assessment

Form RA01 16/10/03

Risk Assessment	4th Year Project – Fast Level Set Segmentation of Biomedical Images using GPUs			Page 1 of 1
In Building	Oxford E-Research Centre			
Assessment undertaken	Hormuz Mostofi	Signed	Date :	18th November 2008
Assessment supervisor	Julia Schnabel	Signed	Date :	18th November 2008

Hazard	Persons at Risk	Risk Controls In Place	Further Action Necessary To Control Risk
Headache and eyestrain	User	• Taking regular breaks of approx 5 minutes per hour • Calibrating screen properly (brightness and flicker prevention) • Ensuring there is adequate ambient room lighting	Consult Supervisor and advise Departmental Safety Officer if problems persist
Back pain	User	• Adjusting chair properly and ensuring correct seating posture	Consult Supervisor
Upper limb pain	User	• Ensure correct seat height • Use wrist rest • Forearms horizontal and level with desk surface	Consult Supervisor
Lower limb pain	User	• Allow room for legs under desk and/or place footrest	Consult Supervisor
Electrical shock from computing equipment	User	• Ensure all electrical equipment is PAT tested by Electronics	Consult Supervisor to check validity of PAT test and label

Your E-mail Address ……Checked by ..... date ……..

(D J Reed)